Resource Allocation and Basestation Placement in Downlink Cellular Networks Assisted by Multiple Wireless Powered UAVs

Sixing Yin, *Member, IEEE*, Lihua Li, *Member, IEEE*, and F. Richard Yu, *Fellow, IEEE*

***Abstract*—In this paper, we focus on a downlink cellular network, where multiple UAVs serve as aerial basestations to provide wireless connectivity to ground users through frequency division multi-access (FDMA) scheme. The UAVs are exclusively powered by a wireless charging station located on the ground following save-then-transmit protocol. In such a UAV-assisted cellular network, joint optimization for user association, resource allocation and basesation placement are investigated to maximize the downlink sum rate. The problem is formulated as a mixed integer optimization problem and is thus challenging to solve. We propose an efficient solution based on alternating optimization, by iteratively solving one of the three subproblems (i.e., user association, resource allocation and basesation placement) with the other two fixed. Specificly, user association is solved as a standard linear programming problem by relaxing the binary association indicators into continuous variables. For basestation placement and resource allocation, we resort to successive convex optimization technique, which iteratively solves a lower-bound problem. After iteratively solving the three subproblems, we further propose an algorithm based on penalty method and successive convex optimization to make the association indicators feasibly binary. We conduct comprehensive experiments for the optimal solution to the three subproblems with insightful results. We also show that the optimal downlink sum rate cannot be always enhanced by deploying more UAVs due to non-negligible tradeoff between energy/communication sources and co-channel interference. Moreover, the proposed solution outperforms a baseline strategy leveraged from an existing work, especially with favorable channel condition and sufficient frequency resources.**

***Index Terms*—UAV-assisted communications, wireless powered communication networks.**

I. Introduction

DUE to increasing demand for seamless connectivity and high-quality data transmission in the next-generation wireless communications, enhancing existing cellular networks by simply investing in more terrestrial infrastructures (e.g., ultra-dense deployment of small cells) has been no longer a cost-effective solution for CAPEX/OPEX. Moreover, terrestrial infrastructures are vulnerable to unexpected damage (e.g., caused by natural disasters), in which case it could be difficult to rapidly recover the interrupted links. For these reasons, effort on network deployment has been refocused on shift from two-dimensional ground plane to three-dimensional space.

Recently, wireless communications aided by unmanned aerial vehicles (UAVs, also known as drones) have received significant attention due to their maneuverability, flexible deployment and cost effectiveness [1]. Thus, conventional cellular networks have been extended toward 3D architecture for coverage enhancement [2] and relevant applications can be also found in ad-hoc networks [3], D2D networks [4] and even cloudlet-aided recommendation systems [5]. In particular, UAVs that serve as aerial basestations can be deployed to provide wireless connectivity in areas with insufficient infrastructures, e.g., traffic offloading for overloaded basestations, which is also one of the key scenarios that need to be effectively addressed by the fifth generation (5 G) wireless systems [6]. Compared to conventional ground infrastructures, such flexible deployment makes aerial basestations able to find better spots for reliable transmission and more robust against stringent environments. Therefore, deploying aerial basestations for temporary link re-establishing is also a promising solution for emergency communication applications, e.g., post-disaster operations.

Industrial leading companies have launched several pilot projects for UAV-enabled wireless communications. In Google's Project Loon, high-altitude balloons are placed in the stratosphere to provide wireless connection with up to 100 Mbit/s for rural areas [7]. Similarly, effort has been made by Facebook in Project Aquila to provide airborne connectivity by deploying high-altitude aircraft [8]. Moreover, the 3 rd Generation Partnership Project (3GPP) has also been investigating communications in the sky with aerial vehicles supported by long term evolution (LTE) [9].

Despite the notable advantages over conventional infrastructure-based wireless communications, UAV-assisted wireless communications are still facing many new challenges, e.g., stringent latency and security requirements for supporting safety-critical functions, and new communication protocols that take into account sparse and intermittent network connectivity resulted from the high mobility environment of UAV systems [1].

Manuscript received October 17, 2019; accepted December 10, 2019. Date of publication December 19, 2019; date of current version February 12, 2020. This work was supported in part by the National Science and Technology Major Project of the Ministry of Science and Technology of China under Grant 2018ZX03001-031 and in part by the National Natural Science Foundation of China under Grant 61629101. The review of this article was coordinated by Dr. F. Tang. *(Corresponding author: Sixing Yin.)*

S. Yin and L. Li are with the Beijing Key Laboratory of Network System Architecture and Convergence, Beijing University of Posts and Telecommunications, Beijing 100876, China (e-mail: yinsixing@bupt.edu.cn; lilihua@bupt.edu.cn).

F. R. Yu is with the Department of Systems and Computer Engineering, Carleton University, Ottawa, ON K1S 5B6, Canada (e-mail: richard.yu@carleton.ca).

Digital Object Identifier 10.1109/TVT.2019.2960765

Limited on-board battery is also one of those challenges. In addition to energy consumed by wireless communications, UAVs also inevitably incur mechanical energy consumption to support their operations, which is usually much higher in practice. However, their on-board batteries are usually of low capacity in consideration of aircraft's size and weight. To tackle such a critical issue, there have been existing works that focus on energy consumption trade-off [10] or energy efficiency improvement [11].

Alternatively, exploring other energy sources is also an important option. Wireless power transfer (e.g., microwave that travels hundreds of meters) has recently received extensive attention since it is able to utilize energy carried by radio signal as energy replenisher to wireless networks. Therefore, a new paradigm termed wireless powered communication networks (WPCN) has been proposed, where wireless devices are able to be powered over the air by dedicated wireless power transmitters [12]. Compared to conventional battery-powered communication networks, WPCN is able to efficiently tackle the difficulties in manually replacing/recharging batteries, especially for areas in harsh condition [13]. As a research upsurge, there have been volumes of papers that focus on performance enhancement [14], [15], user cooperation [16], [17], as well as potential applications in association with other leading-edge techniques [18], [19].

Compared to near-field wireless power transfer with inductive, capacitive, or resonant coupling, far-field wireless power transfer based on radio signal can better fit UAV-aided communications with high altitude due to its long transfer range up to tens of kilometers [20]. Thus, with the recent advance in wireless power transfer [21], there have been reports on solutions for wirelessly powering drones without batteries [22], [23], and even pioneer work on UAV-enabled wireless powered communication network, where a UAV serves as a wireless charger for ground users [24]. Though at its early stage, it is still foreseeable that long-distance wireless power transfer could allow for farming solar power from orbit [25].

In addition, to take the advantage of UAVs' flexible location adjustment, a great deal of research work on aerial basestation placement can be found for performance enhancement in UAV-assisted wireless networks. In terms of coverage maximization, the optimal altitude of a single low-altitude UAV is investigated to tackle the tradeoff between radio propagation loss of line-of-sight probability. Similarly, The authors in [26] focus on deployment for multiple UAVs with directional antennas. The authors in [27] study a similar problem from a different angle, where the number of UAV-mounted mobile basestations is minimized while ensuring that all the ground terminals can lie within the communication range of at least one mobile basestation. Besides, [28] explores three-dimensional space and investigates the placement problem for aerial basestations to maximize the maximum number of users covered by a drone-cell. In [29], deployment for both aerial and ground basestations is investigated to minimize the average network delay. The authors in [30] improve the throughput of a heterogeneous network by dynamically adjusting locations of full-duplex-enabled UAVs. Considering user mobility, the authors in [31] design a novel strategy for aerial basestation placement based on reinforcement learning. In fact, for UAV-assisted communications with wireless power transfer, UAV placement is even more important since the UAVs' locations affect performance of not only information transfer but also power transfer.

Based on such motivations, in this paper, we focus on a downlink cellular network, where multiple UAVs that are remotely powered by a wireless charging station located on the ground and serve as aerial basestations to provide wireless connectivity to ground users through frequency division multi-access (FDMA) scheme (i.e., ground users are served on different orthogonal channels). Undoubtedly, such a cellular network with wireless powered UAVs necessitates carefully designed resource allocation scheme (e.g., downlink power allocation as well as UAV and channel assignment). We focus on timeslot mode for wireless charging and downlink transmission, i.e., in each uniform-length timeslot, the UAVs are first recharged by the charging station on the ground and then perform downlink transmission for the ground users. Therefore, scheduling between wireless charging and downlink transmission must be taken into account due to the non-trivial tradeoff between the two that share the same timeslot. In addition to resource allocation, choice of basestation placement is also non-negligible since locations of the UAVs affect both wireless charging performance and downlink channel conditions. Therefore, in such a scenario, we study joint optimal design for resource allocation and basestation placement to maximize the downlink sum rate. The main contributions of this paper are summarized as follows:

1) We propose a paradigm for wireless communication systems aided by wireless powered UAVs that serve as aerial basestations and investigate the downlink sum rate maximization problem by jointly optimizing resource allocation and basestation placement.
2) For single-UAV case, we investigate the optimal choices for downlink power allocation and wireless charging duration and reformulate the downlink sum rate maximization problem as a fractional programming one.
3) For multi-UAV case, we decomposed the downlink sum rate maximization problem into three subproblems (i.e., user association, basestation placement and resource allocation), and alternately solve each one given the other two with a proposed algorithm.

The rest of this paper is organized as follows. In Section II, the cellular network aided by wireless powered UAVs is described in detail and the downlink sum rate maximization problem is mathematically formulated. In Section III, solution for the single-UAV case is derived with in-depth analysis. In Section IV, problem for the general multi-UAV case is decomposed into three subproblems for user association, basestation placement and resource allocation, which are separately investigated. Simulation results are presented in Section V and we conclude this paper in Section VI.

II. System Model and Problem Formulation

As shown in Fig. 1, we focus on a downlink cellular network, where M UAVs hovering in the air at altitude H operate as aerial basestations to serve K ground users located in an inaccessible area without communication infrastructures (e.g.,

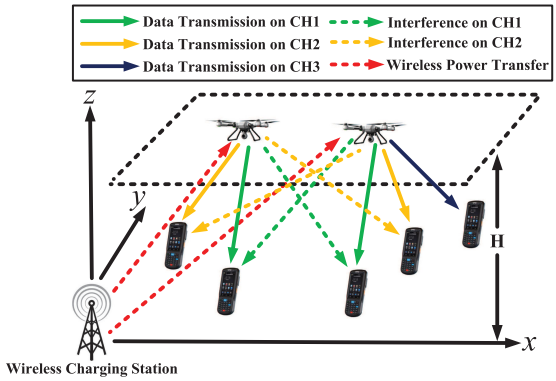

Fig. 1. A downlink cellular network with multiple UAVs as aerial basestations, which are powered by a wireless charging station on the ground.

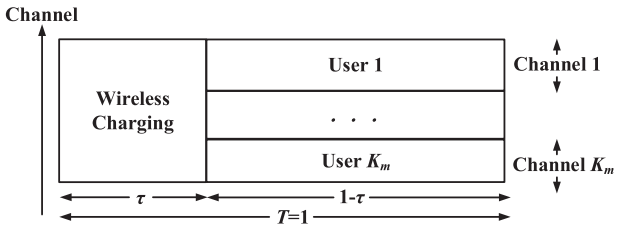

Fig. 2. Timeslot framework for wireless charging and FDMA resource sharing.

a disaster zone).[1] All the UAVs are powered exclusively by a wireless charging station located on the ground to support sustainable operation. We assume that the UAVs operate in timeslot mode and follow the save-then-transmit protocol [32], i.e., in each timeslot with duration T, which is normalized as $T = 1$ throughout this paper, the UAVs harvest energy from the wireless charging station in the first place (the duration is denoted by τ) and then perform downlink transmission for all the ground users. We focus on FDMA for orthogonal resource sharing among ground users, i.e., the downlink transmission is carried out on N orthogonal channels. The timeslot framework for an individual UAV m that serves K_m users is shown in Fig. 2, where each ground user is served on an individual channel. In addition, we assume that the entire communication resources are sufficient to serve all the ground users (i.e., $MN \geq K$) and adjacent channel interference can be eliminated by existing techniques (e.g., setting up guard band).

Without loss of generality, we consider a three dimensional Cartesian coordinate system with the wireless charging station located at the origin and locations of UAV m and ground user k are denoted by $[x_m, y_m, H]$ and $[x_k, y_k, 0]$, respectively. We assume that channels between all the UAVs and all the ground users are dominated by line-of-sight (LOS) links. Therefore, within each timeslot, channel power gain is given by

$$h_{km} = \frac{\beta}{(d_{km})^{\alpha}} = \frac{\beta}{\left[(x_k - x_m)^2 (y_k - y_m)^2 + H^2\right]^{\alpha/2}} \quad (1)$$

[1]The terms "UAV" and "aerial basestation" are interchangeable in this paper.

for channel between UAV m and user k.[2] Similarly, power gain of channel between the aerial basestations and the wireless charging station is given by

$$h_m = \frac{\beta}{(d_m)^{\alpha}} = \frac{\beta}{[x_m^2 + y_m^2 + H^2]^{\alpha/2}} \quad (2)$$

In both (1) and (2), β denotes the channel power gain at the reference distance (e.g., one meter), $\alpha \geq 2$ denotes the path loss exponent and d_{km} denotes the distance between UAV m and ground user k, and d_m denotes the distance between UAV m and the wireless charging station, respectively. Thus, for UAV m, the total energy harvested from the wireless charging station in each timeslot amounts to $P_w h_m \tau$, where P_w refers to the transmit power of the wireless charging station.[3] Let P_h denote the hovering power consumption for each aerial basestation and we assume that $P_w h_m > P_h$ for $m = 1, \ldots, M$ always holds to ensure a sufficient amount of harvested energy, i.e., the UAVs should be able to afford at least their hovering energy consumption by harvesting energy for the entire timeslot ($\tau = 1$).

In such a downlink cellular network, both resource allocation and basestation placement are of great importance for the overall performance. Wireless charging duration balances the aerial basestations' harvested energy and effective transmission performance. The UAV-user-channel association and the UAVs' power allocation among channels must be carefully designed since co-channel interference is non-negligible to the overall performance. Moreover, all the UAVs must be properly located to tackle the tradeoff between energy harvesting performance and downlink channel condition. To this end, we focus on joint optimization for resource allocation and basestation placement to maximize the downlink sum rate and such a problem can be formulated as

$$\begin{aligned}
\max_{\boldsymbol{\rho}, \boldsymbol{p}, \tau, [\boldsymbol{x}, \boldsymbol{y}]} \quad & (1-\tau) \sum_{k=1}^{K} \sum_{m=1}^{M} \sum_{n=1}^{N} \rho_{kmn} \log\left(1 + \frac{p_{mn} h_{km}}{\sigma + \sum_{j \neq m} p_{jn} h_{kj}}\right) \\
\text{s.t.} \quad & P_h + (1-\tau) \sum_{n=1}^{N} p_{mn} \leq P_w h_m \tau, \quad \forall m \\
& \sum_{m=1}^{M} \sum_{n=1}^{N} \rho_{kmn} = 1, \quad \forall k \\
& p_{mn} \geq 0, \sum_{k=1}^{K} \rho_{kmn} \leq 1, \quad \forall m, n \\
& 0 \leq \tau \leq 1, \rho_{kmn} \in \{0, 1\}, \quad \forall k, m, n
\end{aligned} \quad (3)$$

where $[\boldsymbol{x}, \boldsymbol{y}] = \{[x_1, y_1], \ldots, [x_M, y_M]\}$, the binary variable $\boldsymbol{\rho} = \rho_{kmn}$ serves as the association indicators for channel assignment and UAV association for each ground user (i.e., $\rho_{kmn} = 1$ means user k is served by UAV m on channel n

[2]We assume that all the N channels are adjacent on frequency band such that difference in channel power gain resulted from different frequency bands can be neglected.

[3]In this paper, we assume the UAVs' energy conversion efficiency is independent of their input power level while non-linear energy harvesting model resulted from the energy harvesting circuits is not taken into account [33].

while $\rho_{kmn} = 0$ means otherwise), $\boldsymbol{p} = p_{mn}$ specifies power allocation among different channels for each UAV (i.e., p_{mn} denotes UAV m's downlink transmission power on channel n) and σ denotes the uniform channel noise power. The first group of constraints in (3) is to avoid power deficit for each UAV while the second and third groups of constraints ensure that each ground user is uniformly served with one "resource block" (i.e., served by one UAV on one single channel at a time) and each resource block is occupied for serving at most one ground user.

Obviously, (3) is a mixed integer non-convex optimization problem with both continuous and binary variables, which is thus challenging and cannot be simply solved with standard convex optimization techniques. In the following sections, we resort to alternating optimization (also known as block descent method) to solve the problem by decomposing (3) into three subproblems for user association, resource allocation and basestation placement, respectively. Each of the three groups of variables (i.e., association indicators $\boldsymbol{\rho}$, downlink power allocation and wireless charging duration $\boldsymbol{p}$ and τ, as well as the UAVs' locations $[\boldsymbol{x}, \boldsymbol{y}]$) is alternatively optimized given the other two. Based on solutions to the three subproblems, the downlink sum rate of the cellular network can be thus iteratively improved until convergence.

III. Single-UAV Case

In this section, we first focus on a special case of the problem in (3), where only one UAV serves as the aerial basestation in the cellular network. Likewise, we assume that the frequency band resources are sufficient, i.e., $K = N$, such that each user can be assigned with one individual channel and co-channel interference never exists. Therefore, the original problem can be simplified as

$$\begin{aligned} \max_{\boldsymbol{p},\tau,[x,y]} \quad & (1-\tau)\sum_{n=1}^{N}\log\left(1+\frac{p_n h_n}{\sigma}\right) \\ \text{s.t.} \quad & P_h + (1-\tau)\sum_{n=1}^{N} p_n \le P_w h \tau \\ & p_n \ge 0, \quad \forall n, 0 \le \tau \le 1 \end{aligned} \tag{4}$$

where UAV index m, association indicators $\boldsymbol{\rho}$ and the co-channel interference term are removed from (3) since only a single UAV is taken into account.

We first investigate the optimal design for power allocation and wireless charging duration given the aerial basestation's location. It is easy to find that in (4), τ can be eliminated by making the equality hold for the first constraint, i.e., $\tau = (P_h + \sum_{n=1}^{N} p_n)/(P_w h + \sum_{n=1}^{N} p_n)$, since the objective is always monotonically decreasing with τ. Thus, (4) can equivalently simplified as a power allocation problem:

$$\begin{aligned} \max_{\boldsymbol{p}} \quad & \frac{P_w h - P_h}{P_w h + \sum_{n=1}^{N} p_n}\sum_{n=1}^{N}\log(1+p_n h_n) \\ \text{s.t.} \quad & p_n \ge 0, \quad \forall n = 1, \ldots N \end{aligned} \tag{5}$$

where σ is removed for simplicity (or $\sigma = 1$) such that h_n equivalently denotes the power-gain-to-noise-ratio of channel n. Apparently, (5) falls into a typical fractional programming problem and can be solved by first solving

$$\max_{\boldsymbol{p}\ge\boldsymbol{0}} \quad f(\boldsymbol{p}) = \sum_{n=1}^{N}\log(1+p_n h_n) - \theta\left(P_w h + \sum_{n=1}^{N} p_n\right) \tag{6}$$

Given θ, the optimal solution to (6) can be derived as a function of θ and the optimal sum rate can be obtained by solving $f(\boldsymbol{p}^*(\theta)) = 0$.

Obviously, (6) is a convex optimization problem due to its concave-minus-affine objective function and can be readily solved through parallel decomposition, i.e., solving

$$\max_{p_n\ge 0} \quad \log\left(1+p_n h_n\right) - \theta p_n \tag{7}$$

for $n = 1, \ldots, N$. The optimal solution to (6) given θ can be derived by solving its first-order derivative equation, which is given by

$$p_n^*(\theta) = \left[\frac{1}{\theta} - \frac{1}{h_n}\right]^+ \tag{8}$$

where $[x]^+ = \max\{0, x\}$. Obviously, (8) has a water-filling form, where $1/\theta$ also serves as the "water level" and can be uniquely determined by solving $f(\boldsymbol{p}^*(\theta)) = 0$.

Without loss of generality, we assume that h_n is sorted in descending order, i.e., $h_1 \ge \ldots \ge h_L \ge \theta \ge h_{L+1} \ge \ldots \ge h_N$, where $L \in \{1, \ldots, N\}$ is an integer that satisfies $h_L \ge \theta$. According to (8), we have

$$\begin{aligned} f(\boldsymbol{p}^*(\theta)) &= \sum_{n=1}^{L}\log\left(1+p_n^*(\theta)h_n\right) - \theta\left(P_w h + \sum_{n=1}^{L} p_n^*(\theta)\right) \\ &= -L\log\theta + \left(\sum_{n=1}^{L}\frac{1}{h_n} - P_w h\right)\theta + \sum_{n=1}^{L}\log h_n - L \end{aligned} \tag{9}$$

Then following Lemma 1 in [34], solution to $f(\boldsymbol{p}^*(\theta)) = 0$ is given by

$$\theta = \frac{W(a\mathrm{e}^b)}{a} \tag{10}$$

where a and b are defined as

$$\begin{cases} a = \dfrac{1}{L}\left(P_w h - \sum_{n=1}^{L}\dfrac{1}{h_n}\right) \\ b = \dfrac{1}{L}\sum_{n=1}^{L}\log h_n - 1 \end{cases} \tag{11}$$

and $W(\cdot)$ is the Lambert W function. Therefore, solving $f(\boldsymbol{p}^*(\theta)) = 0$ is equivalent to finding an integer $L \in \{1, \ldots, N\}$ such that θ in (10) is feasible, i.e., $h_{L+1} \le \theta \le h_L$. One can always enumerate all the integers within $[1, N]$ to find such an integer. However, since the Lambert W function cannot be expressed in terms of elementary functions and its computational complexity is not negligible, straightforward enumeration over $L \in \{1, \ldots, N\}$ for (10) is still computational costly due to repeated computation for the Lambert W function. To reduce the computational cost and search space, we take a further look at (10).

According to the property of the Lambert W function, θ is positive only when $a \geq 0$, by which $a\mathrm{e}^b > 0$ always holds. Otherwise, $W(a\mathrm{e}^b)$ turns to a double-valued function, or even is undefined if $a\mathrm{e}^b < -1/\mathrm{e}$. Since a is decreasing with L according to its definition, by searching from 1 to N, one can always find L_m that satisfies $a \geq 0$ for $L \in \{1, \ldots, L_m\}$ and $a < 0$ for $L \in \{L_m + 1, \ldots, N\}$, which effectively reduces the search space. To reduce the computational cost, it can be inferred from the feasibility definition of θ that

$$\begin{aligned} & h_{L+1} \leq \theta \leq h_L \\ & \Rightarrow a h_{L+1} \leq W\left(a\mathrm{e}^b\right) \leq a h_{L+1} \\ & \Rightarrow a h_{L+1}\mathrm{e}^{a h_{L+1}} \leq a\mathrm{e}^b \leq a h_L \mathrm{e}^{a h_L} \\ & \Rightarrow \log h_{L+1} + a h_{L+1} \leq b \leq \log h_L + a h_L \end{aligned} \tag{12}$$

Therefore, without repeated computation for the Lambert W function, the feasibility of θ can be verified by enumerating $L \in \{1, \ldots, L_m\}$ and testing with the last group of inequalities in (12).

With L determined, the optimal θ and power allocation can be derived in turn following (10) and (8), respectively, and then the optimal wireless charging duration can be determined by

$$\tau^* = \left(P_h + \sum_{n=1}^{N} p_n^*\right) \Bigg/ \left(P_w h + \sum_{n=1}^{N} p_n^*\right) \tag{13}$$

The next step is to optimize the aerial basestations' locations given power allocation and wireless charging duration. Since solving the basestation placement problem for single-UAV case is quite similar with that for the multi-UAV case, we leave this part to the next section. Please refer to Section IV-B for the detail.

IV. Multi-UAV Case

In this section, we focus on the general case of the problem in (3), where more than one UAVs serve as aerial basestations (i.e., $M \geq 2$). As discussed in Section III, the problem can be decomposed into three subproblems, which are alternately solved such that the downlink sum rate of the cellular network can be iteratively improved. In the following part, the three subproblems are separately investigated.

A. User Association

Given time and power allocation and locations of the aerial basestations, the binary association indicators are first relaxed into continuous variables ranging from 0 to 1 in order to make the problem more tractable. Therefore, the relaxed version of the user association optimization problem can be written as

$$\begin{aligned} \max_{\boldsymbol{\rho}} \quad & (1-\tau)\sum_{k=1}^{K}\sum_{m=1}^{M}\sum_{n=1}^{N}\rho_{kmn}R_{kmn} \\ \text{s.t.} \quad & \sum_{m=1}^{M}\sum_{n=1}^{N}\rho_{kmn} = 1, \quad \forall k \\ & \sum_{k=1}^{K}\rho_{kmn} \leq 1, \quad \forall m, n \\ & 0 \leq \rho_{kmn} \leq 1, \quad \forall k, m, n \end{aligned} \tag{14}$$

where $R_{kmn} = \log[1 + p_{mn}h_{km}/(\sigma + \sum_{j\neq m} p_{jn}h_{kj})]$ refers to the individual rate of user k served by UAV m on channel n. Due to the continuous-variable relaxation, the optimum of (14) serves as an upper bound for that of (3) given time and power allocation and locations of the aerial basestations. Obviously, (14) is a typical linear programming problem and can be efficiently solved via existing optimization techniques, e.g., the simplex method. Since the optimal solution to (14) is not necessarily binary in general, it still needs to be binarized as feasible association indicators after alternating optimization, which will be elaborated in Section IV-E.

B. Basestation Placement

Given user association indicators and power allocation of the aerial basestations, the basestation placement problem can be formulated as

$$\begin{aligned} \max_{[\boldsymbol{x},\boldsymbol{y}]} \quad & (1-\tau)\sum_{k=1}^{K}\sum_{m=1}^{M}\sum_{n=1}^{N}\rho_{kmn}R_{kmn} \\ \text{s.t.} \quad & \frac{1}{[x_m^2 + y_m^2 + H^2]^{\alpha/2}} \geq C_m, \quad \forall m \end{aligned} \tag{15}$$

where constant C_m is defined as

$$C_m = \left(P_h + (1-\tau)\sum_{n=1}^{N} p_{mn}\right) \Bigg/ \beta P_w \tau \tag{16}$$

Obviously, (15) is non-convex since the objective function and the left hand side of the constraint are both non-concave over the location variables $[\boldsymbol{x}, \boldsymbol{y}]$.

By mimicking the trick in [35], the individual rate can be equivalently written as

$$R_{kmn} = R'_{kn} - \log\left(\sigma + \sum_{j\neq m} \frac{p_{jn}\beta}{\left[(x_k - x_j)^2 + (y_k - y_j)^2 + H^2\right]^{\alpha/2}}\right) \tag{17}$$

where

$$R'_{kn} = \log\left(\sigma + \sum_{m=1}^{M} \frac{p_{mn}\beta}{\left[(x_k - x_m)^2 + (y_k - y_m)^2 + H^2\right]^{\alpha/2}}\right) \tag{18}$$

By introducing slack variables $\boldsymbol{D} = \{D_{kj} = (x_j - x_k)^2 + (y_j - y_k)^2, \forall k, j \neq m\}$, (15) can be equivalently written as

$$\begin{aligned} \max_{[\boldsymbol{x},\boldsymbol{y}],\boldsymbol{D}} \quad & (1-\tau)\sum_{k=1}^{K}\sum_{m=1}^{M}\sum_{n=1}^{N}\rho_{kmn} \\ & \times \left(R'_{kmn} - \log\left(\sigma + \sum_{j\neq m}\frac{p_{jn}\beta}{(H^2 + D_{kj})^{\alpha/2}}\right)\right) \end{aligned}$$

$$\text{s.t.} \quad \frac{1}{[x_m^2+y_m^2+H^2]^{\alpha/2}} \geq C_m, \quad \forall m$$
$$D_{kj} \leq (x_j-x_k)^2+(y_j-y_k)^2, \quad \forall k,j \neq m \quad (19)$$

It is easy to find that the second group of constraints in (19) must hold with equality, otherwise we can always increase the objective by increasing the slack variables D_{kj}. Obviously, the problem in (19) is still non-convex due to its non-concave objective and non-convex feasible set formed by the constraints. To efficiently solve (19), we leverage the successive convex optimization technique proposed in [36], by which a lower bound is iteratively maximized with the optimal location update for all the aerial basestations. Let $[\boldsymbol{x^l}, \boldsymbol{y^l}]$ denote the location of UAV m after l rounds of iteration and $[\Delta^l x_m, \Delta y_m^l]$ denote the location offset of UAV m for location update after l rounds of iteration, i.e., $x_m^{l+1} = x_m^l + \Delta^l x_m$ and $y_m^{l+1} = y_m^l + \Delta^l y_m$.

As discussed in Section III-B of [35], R'_{kmn} is convex with respect to $(d_{km})^2$. Since a convex function is globally lower-bounded by its first-order Taylor expansion at any given point [37], the following inequality holds given $[\boldsymbol{x^l}, \boldsymbol{y^l}]$ after l rounds of iteration:

$$R'_{kn} \geq R^b_{kn} \triangleq A^l_{kn} - \sum_{m=1}^{M} B^l_{kmn}\big[\Delta^l x_m\left(\Delta^l x_m + 2\big(x_m^l - x_k\big)\right) + \Delta^l y_m\big(\Delta^l y_m + 2\left(y_m^l - y_k\right)\big)\big] \quad (20)$$

where the positive constants A^l_{kn} and B^l_{kmn} are defined as

$$\begin{cases} A^l_{kn} = \log\left(\sigma + \sum_{m=1}^{M} \dfrac{p_{mn}\beta}{\left[(x_k - x_m^l)^2 + (y_k - y_m^l)^2 + H^2\right]^{\alpha/2}}\right) \\ B^l_{kmn} = \dfrac{\dfrac{\alpha p_{mn}\beta}{2\left[(x_k - x_m^l)^2 + (y_k - y_m^l)^2 + H^2\right]^{\alpha/2+1}}}{\sigma + \sum_{m=1}^{M} \dfrac{p_{mn}\beta}{[(x_k - x_m^l)^2 + (y_k - y_m^l)^2 + H^2]^{\alpha/2}}} \end{cases} \quad (21)$$

Obviously, R^b_{kn} is a concave quadratic function with respect to $[\boldsymbol{\Delta^l x}, \boldsymbol{\Delta^l y}]$ given locations of the aerial basestations $[\boldsymbol{x^l}, \boldsymbol{y^l}]$.

It is easy to find that the right hand side of the second group of constraints in (19) is convex with respect to $[x_j, y_j]$. Then following lower bound approximation with the first-order Taylor expansion, the following inequality holds given the current location $[x_j^l, y_j^l]$:

$$(x_j - x_k)^2 + (y_j - y_k)^2 \geq \left(x_j^l - x_k\right)^2 + \left(y_j^l - y_k\right)^2 + 2\left(x_j^l - x_k\right)\Delta^l x_j + 2\left(y_j^l - y_k\right)\Delta^l y_j \quad (22)$$

Similarly, considering a convex function $f(z) = 1/(A+z)^{\alpha/2}$ for $z > -A$, it always holds that $f(z) \geq 1/A^{\alpha/2} - z/A^{\alpha/2+1}$ since the first-order Taylor approximation of a convex function is a global under-estimator. Therefore, given $[x_{m,l}, y_{m,l}]$ as the current location of UAV m, the following inequality always holds:

$$\frac{1}{\left(d_m^{l+1}\right)^{\alpha}} \geq \frac{1}{\left(d_m^l\right)^{\alpha}} - \frac{\alpha\Delta_m^l}{2\left(d_m^l\right)^{\alpha+2}} \quad (23)$$

where $\Delta_m^l = \Delta^l x_m^2 + \Delta^l y_m^2 + 2x_m^l \Delta x_m^l + 2y_m^l \Delta^l y_m$.

By combining (20), (22) and (23), it can be inferred that given the current locations of the aerial basestations $[\boldsymbol{x^l}, \boldsymbol{y^l}]$ after l rounds of iteration, the optimum of (19) is always lower-bounded by that of the following problem:

$$\max_{[\boldsymbol{\Delta^l x}, \boldsymbol{\Delta^l y}], \boldsymbol{D}} \quad (1-\tau)\sum_{k=1}^{K}\sum_{m=1}^{M}\sum_{n=1}^{N}\rho_{kmn}\times \left[R^b_{kn} - \log\left(\sigma + \sum_{j\neq m}\frac{p_{jn}\beta}{(H^2 + D_{kj})^{\alpha/2}}\right)\right]$$
$$\text{s.t.} \quad \frac{1}{\left(d_m^l\right)^{\alpha}} - \frac{\alpha\Delta_m^l}{2\left(d_m^l\right)^{\alpha+2}} \geq C_m, \quad \forall m$$
$$D_{kj} \leq \left(x_j^l - x_k\right)^2 + \left(y_j^l - y_k\right)^2 + 2\left(x_j^l - x_k\right)\Delta^l x_j + 2\left(y_j^l - y_k\right)\Delta^l y_j, \quad \forall k,j \neq m \quad (24)$$

It can be readily found that the objective in (24) is concave since it is formed by non-negative weighted sum of "concave-minus-convex" functions. Moreover, since the left hand side of the first constraint is concave and both sides of the second constraint are linear, the constraints form a convex set. Therefore, (24) is a convex problem with respect to the location offset $[\boldsymbol{\Delta^l x}, \boldsymbol{\Delta^l y}]$ and slack variables $\boldsymbol{D}$, which can be readily solved via existing optimization techniques (e.g., the interior-point method [38]). Then following the successive convex optimization technique in [36], (15) can be approximately solved by iteratively solving (24) for the optimal location offset and updating the locations of the aerial basestations.

Thus, the algorithm for optimal basestation placement with fixed user association and time and power allocation is summarized in Algorithm 1. Since the optimum of (24) is always upper-bounded by that of (15), which is undoubtedly finite, it can be guaranteed that Algorithm 1 always converges.

C. Resource Allocation

Given user association and locations of the aerial basestations, the problem of resource allocation can be formulated as

$$\max_{\boldsymbol{p},\tau} \quad (1-\tau)\sum_{k=1}^{K}\sum_{m=1}^{M}\sum_{n=1}^{N}\rho_{kmn}R_{kmn}$$
$$\text{s.t.} \quad P_h + (1-\tau)\sum_{n=1}^{N}p_{mn} \leq P_w h_m \tau, \quad \forall m$$
$$p_{mn} \geq 0, \quad \forall m,n \quad (25)$$

Algorithm 1: Basestation Placement Optimization.

1: Initialize the aerial basestations' locations $[x_m^l, y_m^l]$ for $m = 1, \ldots, M$ that satisfies the constraint in (15) and set $l = 0$;
2: **while** Improvement of the lower bound is higher under a predefined tolerance **do**
3: Solve (24) via the interior-point method for the optimal location offset $[\Delta^{l*} x_m, \Delta^{l*} y_m]$ as well as the optimal slack variables D_{kj}^*;
4: Update the aerial basestation's locations by $x_m^{l+1} = x_m^l + \Delta^{l*} x_m$ and $y_m^{l+1} = y_m^l + \Delta^{l*} y_m$ for $m = 1, \ldots, M$;
5: Set $l = l + 1$;
6: **end while**
7: Output $[\boldsymbol{x^l}, \boldsymbol{y^l}]$ as the optimal locations of the aerial basestations.

where the first group of constraints can be simplified as

$$\tau \geq \max_m \frac{P_h + \sum_{n=1}^N p_{mn}}{P_w h_m + \sum_{n=1}^N p_{mn}} \tag{26}$$

Since the objective in (25) is always monotonically decreasing with τ, (25) attains its optimum only when equality holds in (26). Hence, the first group of constraints along with τ can be eliminated and (25) can be equivalently written as

$$\max_{\boldsymbol{p}} \quad \left(\min_m \frac{P_w h_m - P_h}{P_w h_m + \sum_{n=1}^N p_{mn}} \right) \sum_{k=1}^K \sum_{m=1}^M \sum_{n=1}^N \rho_{kmn} R_{kmn}$$
$$\text{s.t.} \quad p_{mn} \geq 0, \quad \forall m, n \tag{27}$$

Similar with the single-UAV case, (27) falls into a typical fractional programming problem and can be solved by first solving

$$\max_{\boldsymbol{p} \geq \boldsymbol{0}} \quad f(\boldsymbol{p}) = \sum_{k=1}^K \sum_{m=1}^M \sum_{n=1}^N \rho_{kmn} R_{kmn} - \theta \left(\max_m \frac{P_w h_m + \sum_{n=1}^N p_{mn}}{P_w h_m - P_h} \right) \tag{28}$$

which can be further written as

$$\max_{\boldsymbol{p} \geq \boldsymbol{0}, r} \quad \sum_{k=1}^K \sum_{m=1}^M \sum_{n=1}^N \rho_{kmn} R_{kmn} - \theta r$$
$$\text{s.t.} \quad r \geq \frac{P_w h_m + \sum_{n=1}^N p_{mn}}{P_w h_m - P_h}, \quad \forall m \tag{29}$$

by introducing a slack variable r. Given θ, the optimal solution to (6) can be derived as a function of θ and the optimal sum rate can be obtained by solving $f(\boldsymbol{p}^*(\theta)) = 0$.

Although the objective in (29) is not necessarily concave, one can still follow the successive convex optimization by iterative approximation. Let $\boldsymbol{p^l}$ denote the UAVs' power allocation after l rounds of iteration. With the trick in [35], R_{kmn} can be rewritten as

$$R_{kmn} = \log \left(\sigma + \sum_{i=1}^M p_{in} h_{ki} \right) - R''_{kmn} \tag{30}$$

where

$$R''_{kmn} = \log \left(\sigma + \sum_{j \neq m} p_{jn} h_{kj} \right) \tag{31}$$

Similarly, since a concave function is globally upper-bounded by its first-order Taylor expansion at any given point [37], the following inequality always holds:

$$R''_{kmn} \leq R^u_{kmn} \triangleq \log \left(\sigma + \sum_{j \neq m} p^l_{jn} h_{kj} \right) + \sum_{j \neq m} E^l_{kj} \left(p_{jn} - p^l_{jn} \right) \tag{32}$$

where the constant E^l_{kj} is defined as

$$E^l_{kj} = \frac{h_{kj}}{\sigma + \sum_{j \neq m} p^l_{jn} h_{kj}} \tag{33}$$

Therefore, given the current power allocation of the aerial basestations $\boldsymbol{p^l}$, the optimum of (6) is always lower-bounded by that of the following problem:

$$\max_{\boldsymbol{p} \geq \boldsymbol{0}, r} \quad \sum_{k=1}^K \sum_{m=1}^M \sum_{n=1}^N \rho_{kmn} \left(\log \left(\sigma + \sum_{i=1}^M p_{in} h_{ki} \right) - R^u_{kmn} \right) - \theta r$$
$$\text{s.t.} \quad r \geq \frac{P_w h_m + \sum_{n=1}^N p_{mn}}{P_w h_m - P_h}, \quad \forall m \tag{34}$$

It can be readily found that the optimum is attained only when equality holds for the constraint, i.e., $r = \max_m (P_w h_m + \sum_{n=1}^N p_{mn}) / (P_w h_m - P_h)$, because the objective is always decreasing with r. Obviously, (34) is a convex problem with concave objective and convex constraints. Therefore, (34) can be readily solved via existing convex optimization techniques (e.g., interior-point method).

The algorithm for solving (29) given θ is summarized in Algorithm 2. Since the optimum of (34) is always upper bounded by that of (29), which is undoubtedly finite, it can be guaranteed that Algorithm 2 always converges. Similar with the single-UAV case, once (29) is solved given θ, the optimal sum rate can be determined by solving $f(\boldsymbol{p}^*(\theta)) = 0$, e.g., via the bisection method.

D. Alternating Optimization

Based on the solutions to the three subproblems, we come up with an iterative algorithm based on alternating optimization to jointly optimize user association, basestation placement and resource allocation, as summarized in Algorithm 3. After association indicators binarization, as discussed in Section IV-E, basestation placement and resource allocation are still alternately optimized to continue improving the downlink sum rate.

Algorithm 2: Algorithm for Solving (28).

1: Initialize the aerial basestations' power allocation $p_{mn} \geq 0$ for $m = 1, \ldots, M$ and $m = 1, \ldots, N$ and set $l = 0$;
2: **while** Improvement of the lower bound is higher under a predefined tolerance **do**
3: Solve (34) via the interior-point method;
4: Set $l = l + 1$ and update the current power allocation with the solution, i.e., $p_{mn}^{l+1} = p_{mn}^{*}$ for $m = 1, \ldots, M$ and $m = 1, \ldots, N$;
5: **end while**
6: Output $\boldsymbol{p}^{\boldsymbol{l}}$ as the optimal power allocation.

Algorithm 3: Alternating Optimization.

1: Initialize the wireless charging duration and the UAVs' power allocation and locations;
2: **while** Improvement of the downlink sum rate is higher than a predefined tolerance **do**
3: Optimize user association with basestation placement and resource allocation via the simplex method;
4: Optimize basestation placement with fixed user association and resource allocation following Algorithm 1;
5: Optimize resource allocation with user association and basestation placement following Algorithm 2;
6: **end while**;
7: Binarize the association indicators following Algorithm 4;
8: **while** Improvement of the downlink sum rate is higher than a predefined tolerance **do**
9: Optimize basestation placement with fixed user association and resource allocation following Algorithm 1;
10: Optimize resource allocation with user association and basestation placement following Algorithm 2;
11: **end while**;
12: Output the association indicators, wireless charging duration, the UAVs' downlink power allocation and locations as the optimal solution to (3).

According to Algorithm 3, it is notable that with the alternating optimization, the global optimum might not be attained for sure. Hence, the optimality performance of Algorithm 3 might be affected by the initial variables settings, e.g., the UAVs' initial locations.

E. Association Indicators Binarization

As previously discussed, the optimal user association indicators derived by solving (14) are in general continuous and still need to be reconstructed as a feasible binary solution after alternating optimization. This is equivalent to solving (14) with the binary constraint replacing the continuous-variable one for $\boldsymbol{\rho}$, which is given by

$$\begin{aligned} \max_{\boldsymbol{\rho}} \quad & (1-\tau)\sum_{k=1}^{K}\sum_{m=1}^{M}\sum_{n=1}^{N}\rho_{kmn}R_{kmn} \\ \text{s.t.} \quad & \sum_{m=1}^{M}\sum_{n=1}^{N}\rho_{kmn} = 1, \quad \forall k \\ & \sum_{k=1}^{K}\rho_{kmn} \leq 1, \quad \forall m, n \\ & \rho_{kmn} \in \{0,1\}, \quad \forall k, m, n \end{aligned} \tag{35}$$

Since the last binary constraint in (35) can be equivalently rewritten as $\rho_{kmn}(1-\rho_{kmn}) = 0$ for $k = 1, \ldots, K$, $m = 1, \ldots, M$ and $n = 1, \ldots, N$, we resort to the penalty method to solve (35). Therefore, it is equivalent to solving

$$\begin{aligned} \max_{\boldsymbol{\rho}} \quad & (1-\tau)\sum_{k=1}^{K}\sum_{m=1}^{M}\sum_{n=1}^{N}\rho_{kmn}R_{kmn} - \omega\rho_{kmn}^{2}(1-\rho_{kmn})^{2} \\ \text{s.t.} \quad & \sum_{m=1}^{M}\sum_{n=1}^{N}\rho_{kmn} = 1, \quad \forall k \\ & \sum_{k=1}^{K}\rho_{kmn} \leq 1, \quad \forall m, n \end{aligned} \tag{36}$$

where constant ω serves as the penalty factor, which is a large positive factor that penalizes the violation for the binary constraint $\rho_{kmn}(1-\rho_{kmn}) = 0$ since the penalty term $-\omega\rho_{kmn}^{2}(1-\rho_{kmn})^{2}$ is always non-positive. It can be proved that the optimum of (36) converges to that of (35) as $\omega \to \infty$.

Obviously, (36) is not convex in its current form. However, the polynomial objective can be rewritten as a "concave-plus-convex" function, which is given by $(1-\tau)\sum_{k=1}^{K}\sum_{m=1}^{M}\sum_{n=1}^{N} -\omega(\rho_{kmn}^{4} + \rho_{kmn}^{2}) + \rho_{kmn}R_{kmn} + 2\omega\rho_{kmn}^{3}$. Likewise, we resort to successive convex optimization since the first-order Taylor approximation of a convex function is a global under-estimator. Let $\rho_{kmn,l}$ denote the user association indicator after l rounds of iteration, then the following inequality

$$\rho_{kmn}^{3} \geq \rho_{kmn,l}^{3} + 3\rho_{kmn,l}^{2}\left(\rho_{kmn} - \rho_{kmn,l}\right) \tag{37}$$

always holds. Therefore, given $\boldsymbol{\rho}^{l}$, the optimum of (36) is always lower-bounded by that of the following problem

$$\begin{aligned} \max_{\boldsymbol{\rho}} \quad & (1-\tau)\sum_{k=1}^{K}\sum_{m=1}^{M}\sum_{n=1}^{N} -\omega\left(\rho_{kmn}^{4} + \rho_{kmn}^{2}\right) \\ & + \left(R_{kmn} + 6\omega\rho_{kmn,l}^{2}\right)\rho_{kmn} - 4\omega\rho_{kmn,l}^{3} \\ \text{s.t.} \quad & \sum_{m=1}^{M}\sum_{n=1}^{N}\rho_{kmn} = 1, \quad \forall k \\ & \sum_{k=1}^{K}\rho_{kmn} \leq 1, \quad \forall m, n \end{aligned} \tag{38}$$

Algorithm 4: User Association Indicator Binarization.

1: Initialize the user association indicators $\rho_{kmn,l}$ for $k = 1, \ldots, K$, $m = 1, \ldots, M$ and $n = 1, \ldots, N$. Set $l = 0$;
2: **while** Improvement of the lower bound is higher under a predefined tolerance **do**
3: Solve (38) via the interior-point method for the optimal updated association indicators $\rho_{kmn,l+1}$ for $k = 1, \ldots, K$, $m = 1, \ldots, M$ and $n = 1, \ldots, N$;
4: Set $l = l + 1$;
5: **end while**
6: Output $\rho_{kmn,l}$ as the optimal binary user association indicators.

in association with (37). It is easy to find that (38) is convex since its objective is concave and constraints are affine. Therefore, it can be readily solved via existing optimization techniques (e.g., the interior-point method). Then following the successive convex optimization technique in [36], (36) can be approximately solved by iteratively solving (38) and updating the user association indicators.

The algorithm for binarizing user association indicators is summarized in Algorithm 4. Since the optimum of (38) is always upper-bounded by that of (36), which is undoubtedly finite, it can be guaranteed that Algorithm 4 always converges.

F. Complexity Analysis

As discussed in previous subsections, alternating optimization in Algorithm 3 involves solving only convex problems, i.e., solving a linear programming problem with the simplex method and solving conventional convex problems with the interior-point method. It is well known that the simplex method has exponential complexity for the worst case [39], which results in complexity of $O(2^{KMN})$ for solving (14).[4]. According to [37], the worst-case complexity of the interior-point method has an order of square root of the inequality constraint number with properly chosen parameters. Therefore, the complexity of solving (24), (34) and (38) (each iteration in Algorithms 1, 2 and 4) are $O(M)$, $O(\sqrt{M})$ and $O(\sqrt{MN})$, respectively. It is noteworthy that the practical running time of Algorithms 1, 2 and 4 still depends on other parameter settings, e.g, the stop criterion. Hence, the practical efficiency of Algorithm 3 will be evaluated in Section V-B.

V. Simulation Results and Discussions

In this section, simulation results for both single-UAV and multi-UAV cases are presented. Specifically, we focus on a 50m×50m square area, where the wireless charging station is located at the origin (left-bottom corner) and ground users are randomly distributed at least 25m away from the wireless charging station. Without otherwise specified, we have $\beta = 1$, $\alpha = 2$, $\sigma = -20$ dB, $P_w = 40$ dB, $P_h = 0$ dB and $H = 20$ m.

[4]There are alternative algorithms with polynomial complexity for solving linear programming problems, e.g., the ellipsoid method. However, the simplex method is still considered as one of the most efficient algorithms in practice in spite of its exponential worst-case complexity [40].

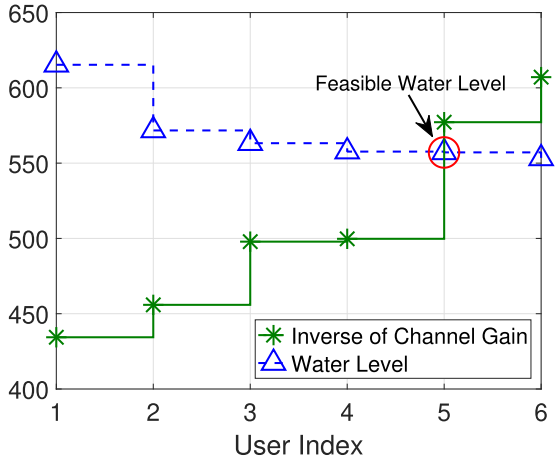

Fig. 3. Comparison between inverse of channel gain and water level. The red circle indicates the unique feasible water level.

A. Single-UAV Case

In this subsection, we first validate the uniqueness of the feasible water level in (10) by focusing on a 20-user cellular network and then evaluate its computational efficiency with different settings of user number. The uniqueness of the water level is validated by comparison between inverse of channel gain and water level with all the possible $L \in \{1, \ldots, 20\}$, which is exemplified in Fig. 3 with user indices sorted with channel gain in descending order. It can be found that instead of searching the entire $L \in \{1, \ldots, 20\}$, at most $L_m = 6$ times of search are necessary since $L > 6$ leads to $a < 0$ and non-existence of θ. Apparently shown in Fig. 3, the feasible water level that satisfies $h_{L+1} \leq \theta \leq h_L$ (or equivalently, $1/h_L \leq 1/\theta \leq 1/h_{L+1}$) is unique as indicated with the red circle, i.e., with $L = 4$, θ falls into the range $[h_5, h_4]$.

To evaluate the computational efficiency of the proposed scheme that reduces the search space for feasible water level, a 1000-time simulation is conducted with the locations of the ground users randomly generated each time. The average search times with different user numbers is shown in Fig. 4. It is notable that the feasibility constraint $a \geq 0$ for the water level significantly reduces the search space, which equals to user number with naive enumeration for all the possible $L \in \{1, \ldots, N\}$. Specially, such search space reduction tends to be more efficient as the user number grows, e.g., the search space is cut down by 72% for 10 users while the cut-down percentage turns to 86% with user number increased to 50.

B. Multi-UAV Case

In this subsection, we focus on the multi-UAV case and simulation results are presented for the three subproblems discussed in Section IV, i.e., user association, resource allocation,

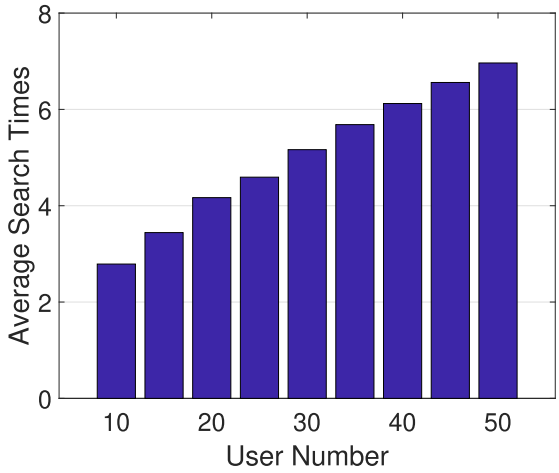

Fig. 4. Average search times for feasible water level versus different user numbers.

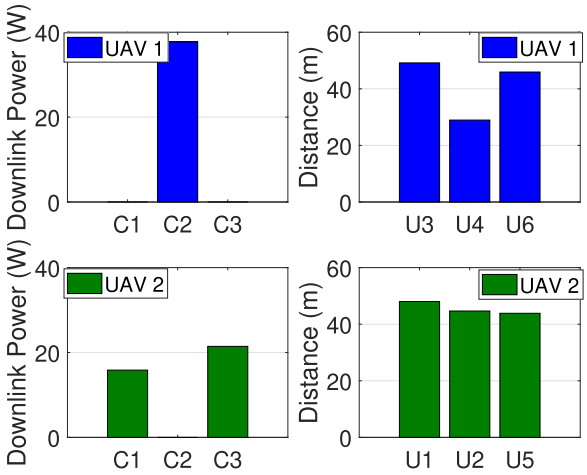

Fig. 6. The optimal power allocation for the two UAVs among three channels and their distance to the associated ground users.

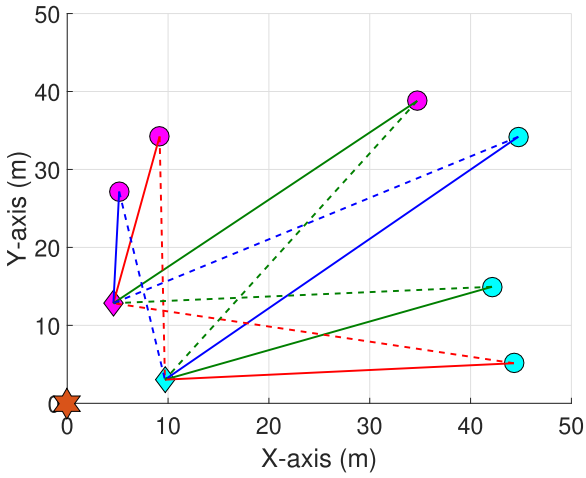

Fig. 5. A typical result for user association. The hexagram represents the wireless charging station, the circles represent the ground users and the diamonds represent the UAVs. The solid lines represent downlink transmission while the dash lines represent co-channel interference. Different channels are identified by solid or dash lines with different colors.

basestation placement, as well as the overall downlink sum rate performance with Algorithm 3.

User Association

In this part, we illustrate the result for the subproblem of user association by considering a downlink cellular network with 6 users, 2 UAVs and 3 channels, where the two UAVs are randomly located less than 25m to the wireless charging station. For each UAV, the energy harvested from the wireless charging station is randomly allocated among the channels for downlink transmission and we have $\tau = 0.5$ for the wireless charging duration. Since both resource allocation and basestation placement are fixed, we directly solve (35) with association indicators binarization following Algorithm 4. A typical result for user association is illustrated in Fig. 5. Here result for user association can be identified by colors. Each user is served by the UAV with the same color and different colors of solid or dash lines signify different channels. Obviously, each user is associated with the closet UAV to guarantee downlink transmission performance. Moreover, in terms of channel assignment, it can be found that co-channel links are as spatially separated as possible in order for interference mitigation. Therefore, as shown in Fig. 5, the solid lines are in general shorter than the dash ones with the same color.

Resource Allocation

In this part, we also focus on a downlink cellular network with 6 users, 2 UAVs and 3 channels to demonstrate the optimal resource allocation given user association and basestation placement. User association is randomly designated under the constraints in (14). To gain more insights, we carefully design the system layout: the two UAVs are intentionally located close to each other and all the ground users are placed with approximately equal distance to their serving UAVs except one (user 4 as shown in Fig. 6), which is significantly closer to its serving UAV. The optimal power allocation of the two UAVs among all the three channels and distance between the UAVs and their associated ground users are illustrated in Fig. 6. Notably, as shown in the left part of Fig. 6, downlink power allocation of the two aerial basestations presents an "interleaved" pattern to avoid co-channel interference. Moreover, we can see that power allocation for each user is in general inversely proportional to its distance to the serving UAV. This is especially the case for UAV 1, which "stakes" all its harvested energy to user 4 that is outstandingly close to it. The optimal charging duration is also investigated by altering the average distance between the aerial basestations and the wireless charging station as well as the transmit power of the wireless charging station, as shown in Fig. 7. It can be found that as the aerial basestations are deployed further away from the wireless charging station, a higher charging duration is preferred to compensate for the deteriorated link for wireless power transfer. Moreover, with higher transmit power of the wireless charging station, shorter charging duration is sufficient to afford the energy consumption

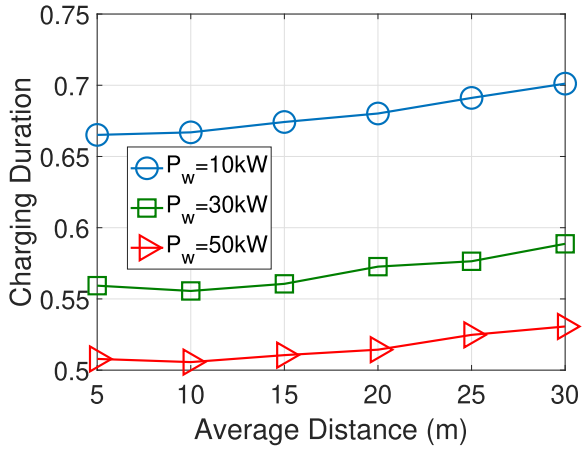

Fig. 7. The optimal charging duration versus average distance between the UAVs and the wireless charging station and its transmit power.

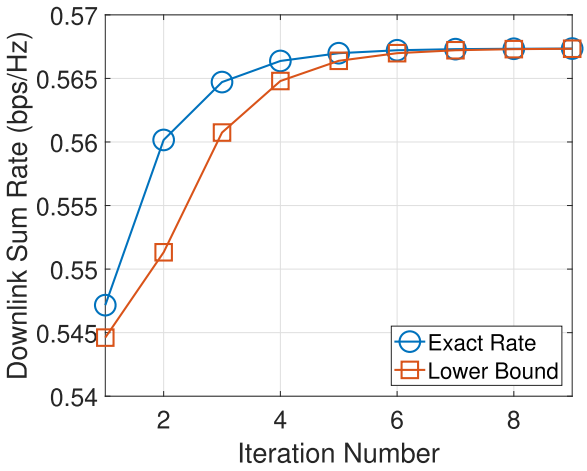

Fig. 8. Downlink sum rate iteration with Algorithm 1.

of the aerial basestations such that more time can be vacated for downlink transmission.

Basesation Placement

In this part, we focus on the performance of Algorithm 1 for basestation placement given user association and resource allocation. Similar with the previous two parts, a downlink cellular network with 6 users, 2 UAVs and 3 channels is considered, where user association is randomly designated under the constraints in (14) and each aerial basestation randomly allocates the harvested energy among all 6 channels with $\tau = 0.5$. To validate the convergence of Algorithm 1, we illustrate iterative evolution of the downlink sum rate following Algorithm 1 as shown in Fig. 8, where the exact downlink sum rate and its lower bound defined by the objective in (24) are both presented. We can see that through the successive convex optimization in Algorithm 1, the downlink sum rate can be iteratively improved and is able to converge effectively within just a few rounds of iteration[5].

[5]The practical convergence rate of Algorithm 1 is closely related to stop criterion, which is the minimum gain of the exact downlink sum rate over the lower bound (0.1% throughout the experiments).

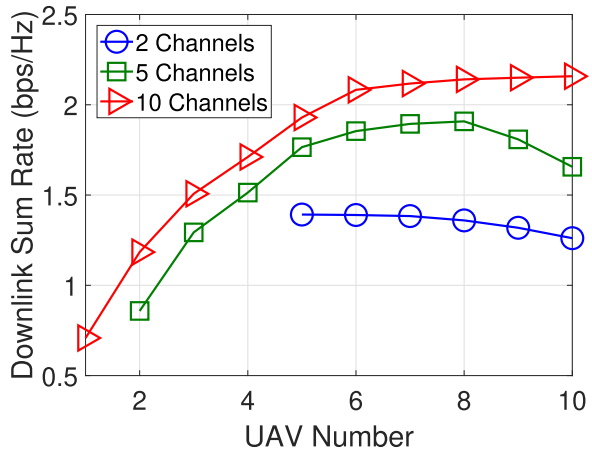

Fig. 9. Optimal downlink sum rate versus UAV number and channel number.

Downlink Sum Rate

In this part, we focus on a downlink cellular network with 10 users, whose locations are randomly generated in the upper-right quadrant of the area and stay unchanged throughout the experiment, and evaluate the performance of downlink sum rate achieved by Algorithm 3. The optimal downlink sum rate with different setting of communication resources (i.e., different number of UAVs and channels) is shown in Fig. 9. Here the three curves are different in size with different channel numbers because the total amount of communication resources must be able to at least suffice for the 10 users. Thus, there must be at least 2 UAVs for 5 channels and the number goes to 5 for 2 channels. In general, it can be found that the optimal downlink sum rate can be improved with more channels. This can be well understood because we can always mitigate co-channel interference with more channels.

Another important finding in Fig. 9 is that, the optimal downlink sum rate cannot be always improved by deploying more UAVs, which is supposed to create more communication resources. In fact, this reveals the pro and con of deploying more UAVs. On one hand, more UAVs are able to create more communication resources, and more importantly, lead to more total energy sources. As shown in Fig. 9, the abundant 10 channels are able to completely prevent co-channel interference from happening such that the increased total energy brought by deploying more UAVs always increases the optimal downlink sum rate. On the other hand, however, excessive UAVs undoubtedly create more interference links, for which even the increased total energy is unable to compensate. This is specially the case for fewer channels. As shown in Fig. 9, with the congested 2 channels, deploying more UAVs is never able to improve the optimal downlink sum rate but increase co-channel interference. In this sense, with limited channels, a proper number of UAVs must be deployed to tackle the tradeoff between total energy sources and co-channel interference, as shown by the curve with 5 channels in Fig. 9.

We also compare the proposed solution with a baseline strategy, which is leveraged from an existing work. In [35], the UAVs serve the ground users in a time division manner and their

trajectories are also taken into account to optimize the fairness performance (common throughput). We replace the objective with the downlink sum rate and assume that a cyclical trajectory for the baseline strategy, i.e., each UAV is first wirelessly charged by hovering at an initial location before beginning its trajectory and then travels back to the location at the end of each timeslot. Hence, with the baseline strategy, the problem for downlink sum rate optimization can be formulated as

$$\begin{aligned}\max_{\boldsymbol{\rho},\boldsymbol{p},[\boldsymbol{x}_l,\boldsymbol{y}_l]} \quad & (1-\tau)\sum_{k=1}^{K}\sum_{m=1}^{M}\sum_{l=1}^{L}\rho_{kml} \\ & \times \log\left(1+\frac{p_{ml}h_{kml}}{\sigma+\sum_{j\neq m}p_{jl}h_{kjl}}\right) \\ \text{s.t.} \quad & P_h+(1-\tau)\sum_{l=1}^{L}p_{ml}\leq P_w h_m \tau, \quad \forall m \\ & \sum_{m=1}^{M}\rho_{kml}\leq 1, \quad \forall k,l \\ & \sum_{k=1}^{K}\rho_{kml}\leq 1, \quad \forall m,l \\ & \rho_{kml}\in\{0,1\}, \quad \forall k,m,l \end{aligned} \tag{39}$$

Similar with [35], the entire time horizon is discretized into L timeslots for ease of derivation. Here p_{ml} denotes the downlink transmission power of UAV m within timeslot l and the binary indicator variable $\rho_{kml}=1$ represents that user k is served by UAV m within timeslot l while $\rho_{kml}=1$ means otherwise. Therefore, the second and third constraints in (39) indicate that within any timeslot, each user is served by at most one UAV and each UAV serves at most one user. In spite of different objectives, the technique proposed in [35] is still applicable to the problem in (39). Since wireless charging for the UAVs is not considered in [35], the wireless charging duration is uniformly set as $\tau=0.5$ for the baseline strategy.

Comparison of downlink sum rate between the proposed solution and the baseline strategy with different settings of path loss exponent is shown in Fig. 10 with 2 UAVs and 10 channels. We can see that the proposed solution always outperforms the baseline strategy and the performance of the two both degrades with a higher path loss exponent. It can be also found that the performance gain of the proposed solution over the baseline strategy tends to shrink due to the excessively unfavorable channel condition. We also compare the proposed solution and the baseline strategy with variable amount of communication resources, i.e., different channel and UAV numbers, as is shown in Fig. 11. Similar with Fig. 9, with the proposed solution, higher downlink sum rate can be achieved with more channels while it cannot be always improved by deploying more UAVs. Differently, the baseline strategy tends to be more immune to co-channel interference with more UAVs deployed. In general, even though the baseline strategy takes the advantage of the UAV's mobility by considering trajectory design, the proposed solution still outperforms it due to a proper choice of user association, downlink power allocation, wireless charging duration and UAV locations. Moreover, it is notable that the performance gap over the baseline strategy is enlarged with more channels (e.g., with 7 channels). Therefore, compared to the time-division baseline strategy, the proposed frequency-division solution is able to benefit the downlink performance in case of sufficient frequency resources, which results in less co-channel interference.

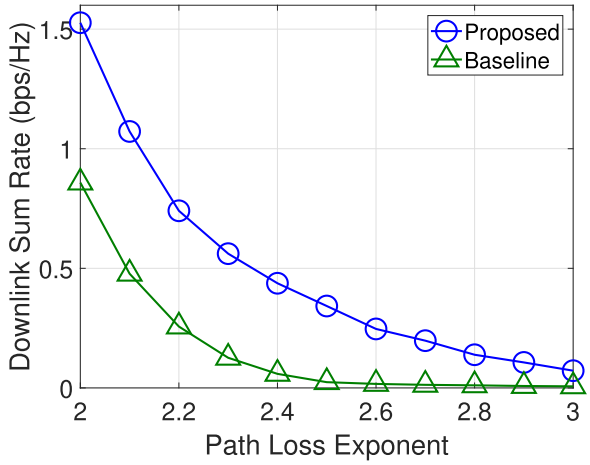

Fig. 10. Comparison for optimal downlink sum rate versus path loss exponent with 2 UAVs and 5 channels.

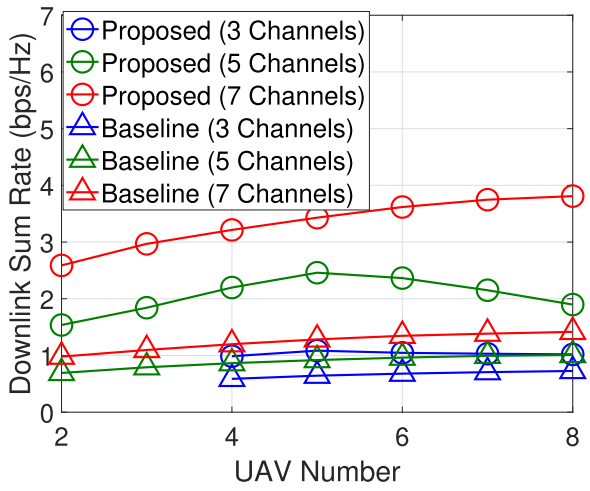

Fig. 11. Comparison for optimal downlink sum rate versus UAV and channel number.

We also evaluate the practical efficiency of Algorithm 3 with average running time of 100-round simulation, where 10 users' locations are randomly generated in the upper-right quadrant of the square area in each round. Average running time with different settings of UAV number and channel number is shown in Fig. 12. It shows that the practical running time of Algorithm 3 increases exponentially with higher problem scale, e.g., more UAVs or channels, and is approximately double with two more channels.

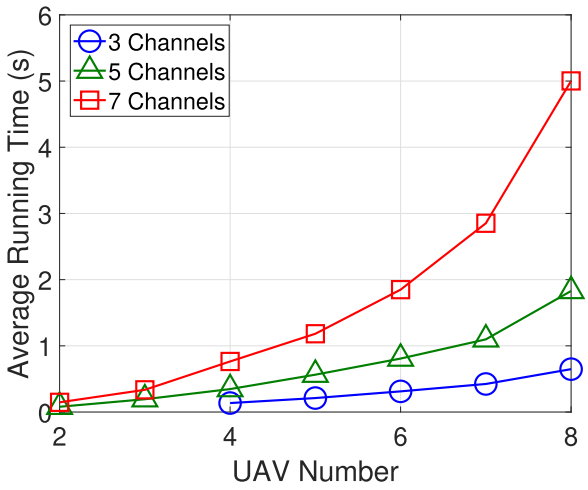

Fig. 12. Average running time with different settings of UAV number and channel number.

VI. Conclusion

In this paper, we considered a downlink cellular network with multiple UAVs that are exclusively powered by a wireless charging station located on the ground and serve as aerial basestations for ground users through FDMA scheme. The problem for downlink sum rate optimization was investigated and formulated as a mixed integer optimization problem. With alternating optimization, the subproblems for user association, basestation placement and resource allocation were separately solved to iteratively improve the optimal downlink sum rate. Specificly, user association is solved as a standard linear programming problem by relaxing the binary association indicators into continuous ones. For basestation placement and resource allocation, we resorted to the successive convex optimization technique, which iteratively solves a lower-bound problem. An algorithm based on penalty method and successive convex optimization was further proposed to binarize the association indicators as feasible ones. Comprehensive experiments were conducted for the optimal solution to the three subproblems with in-depth analysis. Specially, we showed that the optimal downlink sum rate cannot be always enhanced by deploying more UAVs, which reveals its pro and con, i.e., the tradeoff between energy/communication resources and co-channel interference. Moreover, the results also showed that the proposed solution outperforms the baseline strategy, especially in case of favorable channel condition and sufficient frequency resources.

References

[1] Y. Zeng, R. Zhang, and T. J. Lim, "Wireless communications with unmanned aerial vehicles: Opportunities and challenges," *IEEE Commun. Mag.*, vol. 54, no. 5, pp. 36–42, May 2016.

[2] J. Li and Y. Han, "Optimal resource allocation for packet delay minimization in multi-layer UAV networks," *IEEE Commun. Lett.*, vol. 21, no. 3, pp. 580–583, Mar. 2017.

[3] K. Chandrashekar, M. R. Dekhordi, and J. S. Baras, "Providing full connectivity in large ad-hoc networks by dynamic placement of aerial platforms," in *Proc. IEEE Mil. Commun. Conf.*, Oct. 2004, vol. 3, pp. 1429–1436.

[4] F. Tang, Z. M. Fadlullah, N. Kato, F. Ono, and R. Miura, "AC-POCA: Anticoordination game based partially overlapping channels assignment in combined UAV and D2D-based networks," *IEEE Trans. Veh. Technol.*, vol. 67, no. 2, pp. 1672–1683, Feb. 2018.

[5] F. Tang, Z. M. Fadlullah, B. Mao, N. Kato, F. Ono, and R. Miura, "On a novel adaptive UAV-mounted cloudlet-aided recommendation system for lbsns," *IEEE Trans. Emerg. Topics Comput.*, vol. 7, no. 4, pp. 565–577, Oct.–Dec. 2019.

[6] A. Osseiran *et al.*, "Scenarios for 5G mobile and wireless communications: The vision of the METIS project," *IEEE Commun. Mag.*, vol. 52, no. 5, pp. 26–35, May 2014.

[7] "Google loon," 2015. [Online]. Available: https://www.google.com/loon/

[8] "Facebook takes flight," 2015. [Online]. Available: https://www.theverge.com/a/mark-zuckerberg-future-of-facebook/aquila-drone-internet/

[9] "Enhanced LTE support for aerial vehicles," 2017. [Online]. Available: https://www.3gpp.org/dynareport/36777.htm

[10] D. Yang, Q. Wu, Y. Zeng, and R. Zhang, "Energy tradeoff in ground-to-UAV communication via trajectory design," *IEEE Trans. Veh. Technol.*, vol. 67, no. 7, pp. 6721–6726, Jul. 2018.

[11] Y. Zeng and R. Zhang, "Energy-efficient UAV communication with trajectory optimization," *IEEE Trans. Wireless Commun.*, vol. 16, no. 6, pp. 3747–3760, Jun. 2017.

[12] S. Bi, Y. Zeng, and R. Zhang, "Wireless powered communication networks: An overview," *IEEE Wireless Commun.*, vol. 23, no. 2, pp. 10–18, Apr. 2016.

[13] D. Niyato, D. I. Kim, M. Maso, and Z. Han, "Wireless powered communication networks: Research directions and technological approaches," *IEEE Wireless Commun.*, vol. 24, no. 6, pp. 88–97, Dec. 2017.

[14] H. Ju and R. Zhang, "Throughput maximization in wireless powered communication networks," *IEEE Trans. Wireless Commun.*, vol. 13, no. 1, pp. 418–428, Jan. 2014.

[15] Z. Hadzi-Velkov, I. Nikoloska, H. Chingoska, and N. Zlatanov, "Opportunistic scheduling in wireless powered communication networks," *IEEE Trans. Wireless Commun.*, vol. 16, no. 6, pp. 4106–4119, Jun. 2017.

[16] X. Di, K. Xiong, P. Fan, H. C. Yang, and K. B. Letaief, "Optimal resource allocation in wireless powered communication networks with user cooperation," *IEEE Trans. Wireless Commun.*, vol. 16, no. 12, pp. 7936–7949, Dec. 2017.

[17] K. Xiong, C. Chen, G. Qu, P. Fan, and K. B. Letaief, "Group cooperation with optimal resource allocation in wireless powered communication networks," *IEEE Trans. Wireless Commun.*, vol. 16, no. 6, pp. 3840–3853, Jun. 2017.

[18] S. H. Kim and D. I. Kim, "Hybrid backscatter communication for wireless-powered heterogeneous networks," *IEEE Trans. Wireless Commun.*, vol. 16, no. 10, pp. 6557–6570, Oct. 2017.

[19] H. Kim, H. Lee, M. Ahn, H. B. Kong, and I. Lee, "Joint subcarrier and power allocation methods in full duplex wireless powered communication networks for OFDM systems," *IEEE Trans. Wireless Commun.*, vol. 15, no. 7, pp. 4745–4753, Jul. 2016.

[20] I. Krikidis, S. Timotheou, S. Nikolaou, G. Zheng, D. W. K. Ng, and R. Schober, "Simultaneous wireless information and power transfer in modern communication systems," *IEEE Commun. Mag.*, vol. 52, no. 11, pp. 104–110, Nov. 2014.

[21] S. Aldhaher, D. C. Yates, and P. D. Mitcheson, "Design and development of a class EF_2 inverter and rectifier for multimegahertz wireless power transfer systems," *IEEE Trans. Power Electron.*, vol. 31, no. 12, pp. 8138–8150, Dec. 2016.

[22] "This drone could fly forever with wireless power," 2016. [Online]. Available: https://www.popularmechanics.com/flight/drones/a23023/wireless-power-drone/

[23] "Wirelessly powered drone," 2016. [Online]. Available: http://getcorp.com/wirelessly-powered-drone/

[24] L. Xie, J. Xu, and R. Zhang, "Throughput maximization for UAV-enabled wireless powered communication networks," *IEEE Internet Things J.*, vol. 6, no. 2, pp. 1690–1703, Apr. 2019.

[25] "Demo shows drone flying under wireless power," 2016. [Online]. Available: http://fortune.com/2016/09/24/drone-flies-wireless-power/

[26] M. Mozaffari, W. Saad, M. Bennis, and M. Debbah, "Efficient deployment of multiple unmanned aerial vehicles for optimal wireless coverage," *IEEE Commun. Lett.*, vol. 20, no. 8, pp. 1647–1650, Aug. 2016.

[27] J. Lyu, Y. Zeng, R. Zhang, and T. J. Lim, "Placement optimization of UAV-mounted mobile base stations," *IEEE Commun. Lett.*, vol. 21, no. 3, pp. 604–607, Mar. 2017.

[28] R. I. Bor-Yaliniz, A. El-Keyi, and H. Yanikomeroglu, "Efficient 3-D placement of an aerial base station in next generation cellular networks," in *Proc. IEEE Int. Conf. Commun.*, May 2016, pp. 1–5.
[29] M. Mozaffari, W. Saad, M. Bennis, and M. Debbah, "Optimal transport theory for cell association in UAV-enabled cellular networks," *IEEE Commun. Lett.*, vol. 21, no. 9, pp. 2053–2056, Sep. 2017.
[30] L. Zhang, Q. Fan, and N. Ansari, "3-D drone-base-station placement with in-band full-duplex communications," *IEEE Commun. Lett.*, vol. 22, no. 9, pp. 1902–1905, Sep. 2018.
[31] R. Ghanavi, E. Kalantari, M. Sabbaghian, H. Yanikomeroglu, and A. Yongacoglu, "Efficient 3D aerial base station placement considering users mobility by reinforcement learning," in *Proc. IEEE Wireless Commun. Netw. Conf.*, Apr. 2018, pp. 1–6.
[32] S. Luo, R. Zhang, and T. J. Lim, "Optimal save-then-transmit protocol for energy harvesting wireless transmitters," *IEEE Trans. Wireless Commun.*, vol. 12, no. 3, pp. 1196–1207, Mar. 2013.
[33] E. Boshkovska, D. W. K. Ng, N. Zlatanov, and R. Schober, "Practical non-linear energy harvesting model and resource allocation for swipt systems," *IEEE Commun. Lett.*, vol. 19, no. 12, pp. 2082–2085, Dec. 2015.
[34] S. Yin, E. Zhang, J. Li, L. Yin, and S. Li, "Throughput optimization for self-powered wireless communications with variable energy harvesting rate," in *Proc. IEEE Wireless Commun. Netw. Conf.*, Shanghai, China, Apr. 2013, pp. 830–835.
[35] Q. Wu, Y. Zeng, and R. Zhang, "Joint trajectory and communication design for multi-UAV enabled wireless networks," *IEEE Trans. Wireless Commun.*, vol. 17, no. 3, pp. 2109–2121, Mar. 2018.
[36] Y. Zeng, R. Zhang, and T. J. Lim, "Throughput maximization for UAV-enabled mobile relaying systems," *IEEE Trans. Commun.*, vol. 64, no. 12, pp. 4983–4996, Dec. 2016.
[37] S. Boyd and L. Vandenberghe, *Convex Optimization*. Cambridge, U.K.: Cambridge Univ. Press, 2004.
[38] D. P. Bertsekas, *Nonlinear Programming*. Belmont, MA, USA: Athena Scientific, 1999.
[39] R. Shamir, "The efficiency of the simplex method: A survey," *Manage. Sci.*, vol. 33, no. 3, pp. 301–334, Mar. 1987.
[40] A. Schrijver, *Theory of Linear and Integer Programming*. New York, NY, USA: Wiley, 1986.

Sixing Yin received the B.S., M.S., and Ph.D. degrees from the Department of Information and Communication Engineering, Beijing University of Posts and Telecommunications, Beijing, China, in 2003, 2006, and 2010, respectively. He was a Visiting Scholar with the Hong Kong University of Science and Technology in 2009 and worked as a Postdoctoral Fellow with the Beijing University of Posts and Telecommunications from 2010 to 2012. He is currently an Associate Professor with the School of Information and Communication Engineering, Beijing University of Posts and Telecommunications, and a Visiting Scholar with Carleton University, Ottawa, ON, Canada. His research interests include system design and machine-learning-inspired technologies in wireless communications.

Lihua Li received the B.E. and Ph.D. degrees from the Beijing University of Posts and Telecommunications (BUPT), Beijing, China, in 1999 and 2004, respectively. She is currently a Professor with BUPT. She was a Visiting Scholar with Brunel University, London, U.K., in 2006, the University of Oulu, Oulu, Finland, from August 2010 to August 2011, and Stanford University, CA, USA, from April 2015 to April 2016. Her research focuses on wideband mobile communication technologies including MIMO, cooperative transmission technologies, and link adaptation related to new generation mobile communication systems such as 5G and beyond. She has authored or coauthored 92 papers in international and domestic journals and academic conferences, and five books. She has applied for 21 national invention patents and one international patent. She was selected and funded as one of the New Century Excellent Talents by the Chinese Ministry of Education in 2008. She won the second prize of State Technological Invention Award (top-3 China national awards) in 2008 and the first prize of China Institute of Communications Science and Technology Award in 2006 for research achievements of "Wideband Wireless Mobile TDD-OFDM-MIMO Technologies."

F. Richard Yu received the Ph.D. degree from The University of British Columbia, Vancouver, BC, Canada, in 2003. From 2002 to 2006, he was with Ericsson and a start-up in California, USA. He joined Carleton in 2007, where he is currently a Professor. His research interests include cyber-physical systems, connected/autonomous vehicles, security, blockchain, and deep learning. He was the recipient the of IEEE Outstanding Service Award in 2019 and 2016, the IEEE Outstanding Leadership Award in 2013, the Carleton Research Achievement Award in 2012, the Ontario Early Researcher Award in 2011, the Leadership Opportunity Fund Award from CFI in 2009, and many best paper awards. He serves on the editorial boards of several journals, and is the Area Editor for the IEEE COMMUNICATION SURVEYS TUTORIALS and the Lead Series Editor for the IEEE TRANSACTIONS VEHICULAR TECHNOLOGY. He has served as the TPC Co-Chair in numerous conferences. He is a registered Professional Engineer in the province of Ontario, Canada, and a Fellow of the Institution of Engineering and Technology. He is an IEEE Distinguished Lecturer of both Vehicular Technology Society and Communication Society. He is the Vice President (Membership) and an elected member of the Board of Governors of the IEEE Vehicular Technology Society.